O. Nedybaliuk, Ph. D., V. Chernyak, Dr. Sc., Department of Physical Electronics, Faculty of Radiophysics,
E. Martysh, Dr. Sc., Department of Medical Radiophysics, Faculty of Radiophysics, O. Solomenko, post grad. stud.,
Department of Physical Electronics, Faculty of Radiophysics, I. Fedirchyk, stud., Department of Physical Electronics,
Faculty of Radiophysics, Taras Shevchenko National University of Kyiv

PLASMA-LIQUID SYSTEM WITH ROTATIONAL GLIDING ARC AND LIQUID ELECTRODE

In this paper the results of rotational gliding arc investigation with liquid electrode are presented. Emission spectra of plasma that generated by rotational gliding arc with liquid electrode was investigated. Current-voltage characteristics of rotational gliding arc in the range of air flow 0–220 cm³/s were measured. Temperature populations of excited electronic T_e^*, vibrational T_v^* and rotational T_r^* levels were determined. Distribution of temperature along the plasma torch was investigated.
Key words: plasma, rotational gliding arc, liquid electrode, plasma-liquid system, electrical discharge.

Introduction. For today in plasma chemistry, there are three main problems that are related to selectivity of plasma transformation of substances, energy efficiency of plasma technology and the consumption of metallic electrodes material. The problem of selectivity consists in the fact that during the plasma-chemical transformation of substances occur large numbers of chemical reactions. While it is necessary that the reaction occurred that are responsible for the formation of the expected product. This problem is partially solved by using non-equilibrium plasma. Low-temperature plasma is divided by the level of nonequilibrium into two types: plasma with a temperature of heavy components the order of room temperature (dielectric barrier discharge, micro-discharge) and the so-called "warm" plasma with a temperature of ≥ 1000 K.

To support the process of reforming and combustion of hydrocarbon fuels is better to use non-equilibrium "warm" plasma, since the process of reforming requires not only the presence of radicals, but also the appropriate temperature. Moreover, the most promising is the use of plasma at atmospheric pressure or above it.

The problem of energy efficiency of plasma technologies connected with the fact that for the generation of plasma is needed most expensive energy – electric. Therefore, a possible way to solve this problem can be embedding of plasma technologies into the traditional chemical technologies. Plasma must be effectively injected into the reaction chamber. Chemical processes must be managed with help of plasma, using its only as a catalyst.

Atmospheric pressure plasmas can be created by various types of discharges: transverse arc; discharge in gas channel with liquid wall and others. But most of them aren't sufficiently stable. Stabilization of discharge in the high pressure powerful plasmatron is attained by vortex flow of gas [3]. In the low-powered high pressure discharges the reverse vortex flow "tornado" type can be used for the space stabilization [2]. Previous investigations were performed only for discharges with solid-state electrodes. And we have not much information about discharges with liquid electrodes, which were stabilized by vortex and reverse vortex flow of gas. One of the most efficient is the plasma processing in the dynamic plasma-liquid systems using the DC discharge in a reverse vortex gas flow of tornado type with a "liquid" electrode (LE) [5, 6]. Plasma liquid system with rotational gliding arc is a prototype of TORNADO-LE [5, 6], but with some modification, which are interesting for plasma technology.

The peculiarity of the using of plasma-liquid systems to generate plasmas is that they do not require pre-gasification of the liquid. In this regard, the research and development of plasma-liquid systems with a rotational gliding arc and liquid electrode for energy technologies is an urgent task.

Experimental setup. Schematic view of the plasma-liquid system (PLS) with rotational gliding arc is shown in Fig. 1. It consists of a quartz chamber (1) cylindrical shape, which hermetically closed metal top and bottom flanges.
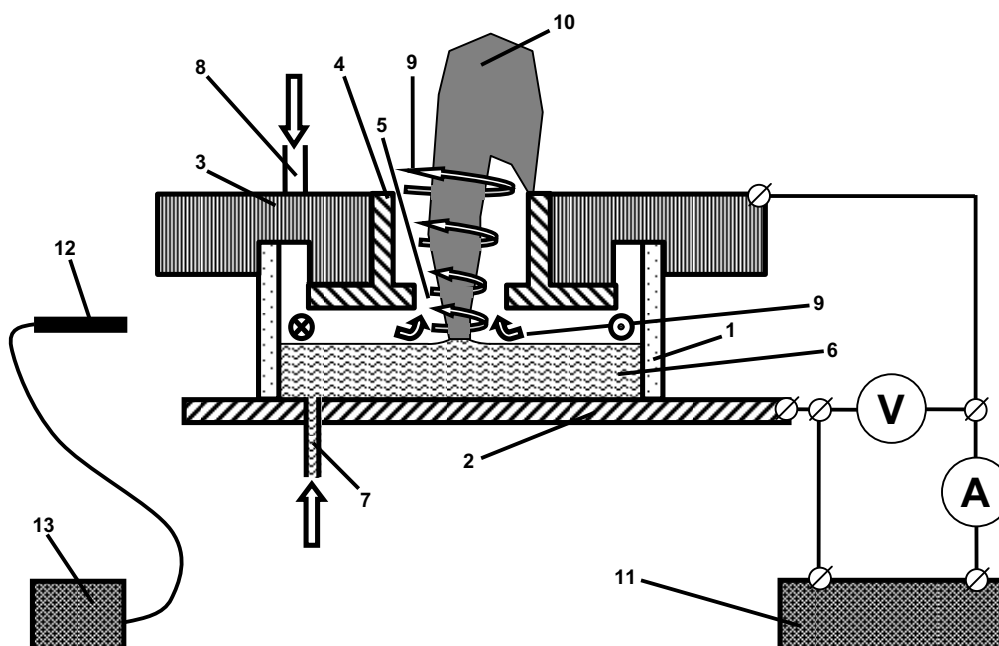

Fig. 1. Schematic diagram of experimental setup

The height of the camera is 30 mm and diameter 90 mm. Bottom flange (2) is made of stainless steel. The upper flange (3) is made of duralumin and contains a copper sleeve (4) which has a hole in the center (5) diameter of 14 mm and a length of 5 mm. Quartz chamber (1) filled with liquid (6), the level of which has been maintained by the injection pump through the aperture (7). Gas inputted into the system through the aperture (8). Gas flow is introduced tangentially to wall of the quartz cylinder (1). Gas, rotating, moved (9) along the surface to the axis of the quartz cylinder (1), where through the aperture (5) comes out. Plasma torch (10) was formed during the discharge burning. One end of plasma torch was located on the surface of the liquid and the other on an external part of the upper flange. Under the influence of the gas flow end of the plasma torch, which was located on the metal surface, rotating, and gliding in the direction of air flow? The voltage between the electrodes was supplied by a power supply (11) DC. The power supply provides voltages up to 7 kV. In this system can be realized two modes of operation: liquid (LC) and solid cathode (SC) cathode.

Emission spectroscopy was used for diagnostics of plasma. Emission spectra were registered using a spectral device that consists of an optical fiber (12) and spectrometer S-150-2-3648 USB (13). This spectrometer allows registering the emission spectra in the wavelength range 200–1000 nm.

Photograph of plasma-liquid system with rotational gliding arc with liquid electrode are shown in Fig. 2. The working fluid was distilled water, the air flow was 220 cm^3/s, current – 360 mA, voltage – 2 kV.
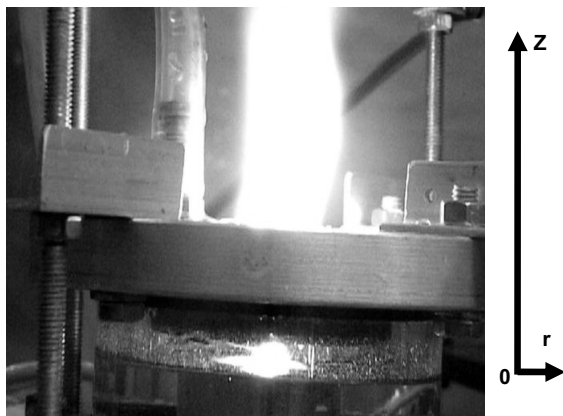

Fig. 2. Photo of plasma-liquid system with rotational gliding arc. Working fluid - distilled water, air flow – 220 cm^3/s, current – 360 mA, voltage – 2 kV. Mode – "solid" cathode

The distance from the surface of liquid to the upper flange – 5 mm. Breakdown of the gas gap occurred in air flow (220 cm^3/s) and a maximum voltage (7 kV) of power supply. Increased airflow lowers the distance between the liquid and the top flange, due to the formation of a cone of liquid on its surface. The gas gap occurred breakdown when the distance reached a certain critical value of. However, after the breakdown of the discharge was burning even in the absence of airflow (0 cm^3/s). Plasma torch was formed outside of the reactor after the breakdown of the gas gap. Length torch initially increased with increasing air flow, reaching a length of about 150 mm by air flow 165 cm^3/s, and then with increase airflow length of torch began to decrease.

Results and discussion. The current-voltage characteristics of the discharge at different airflows are shown in Fig. 3. Mode – "solid" cathode. In the absence of airflow with increasing current voltage unchanged. For air flow 55 cm^3/s at low currents (220 mA) voltage unchanged. The voltage is increased with increasing of current in the range 220–280 mA. The voltage does not change its value at the currents greater than 280 mA. Absolute value of the voltage increased with increasing of airflow (55-165 cm^3/s) but the behavior was similar to the current-voltage characteristics for the air flow of 55 cm^3/s. The voltage was increased with increasing of current and then was voltage saturation. The current-voltage characteristic at airflow 220 cm^3/s has a region where voltage grows, saturates, and then at current of 380 mA began to decrease (Fig. 3). Minimum current at discharge burning was increased with increasing of airflow. The ballast resistance was not used. This may be due to a peculiarity of the impact of air flow to the discharge burning process.

Typical emission spectra of plasma in plasma-liquid system with rotational gliding arc are shown in Fig. 4.
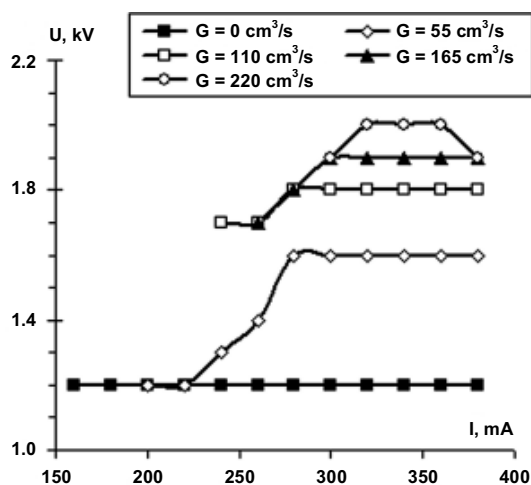

Fig. 3. Current-voltage characteristics of rotational gliding arc

Emission spectra were measured at the regime SC, current 360 mA, voltage 2 kV, air flow 220 cm^3/s. Bands of hydroxyl (OH), lines of hydrogen (H), and multiplets of oxygen (O) are present on emission spectrum of plasma inside ($Z = 2.5$ mm) of plasma-liquid system (Fig. 4.a). Bands of hydroxyl (OH) and lines of copper (Cu) are present on emission spectrum of plasma outside ($Z = 30$ mm) of plasma-liquid system (Fig. 4.b). The plasma torch increases with presence of water. This may be due to the fact that plasma generates detonating gas, which burning increases the plasma torch.

It is obviously that rotational gliding arc plasma discharge, which has been chosen as the basis of our work, has its roots in a LE "tornado" system [5, 6], as can be seen in Fig. 1. As it was shown in [1], the voltage in gliding arc in humid air rather steeply increases with increasing the air flow rate. We have similar effect in our system. But the low intensity of electrode material lines outside PLS and their absence inside (Fig. 4), demonstrates the increasing of electrodes life-time in the RGA plasma discharge. The new state of system can be stable for an indefinite amount of time. So, significant advantage of this system is long lifetime of electrodes.

Temperature T_e^* population of excited electronic levels of the hydrogen atoms H was determined by the method of relative intensities (by two lines H_α – 656.3 nm and H_β – 486.1 nm). Temperature population of excited electronic levels of oxygen atoms O were determined by the Boltzmann diagrams method (777.2 nm, 844.6 nm, 926.6 nm).
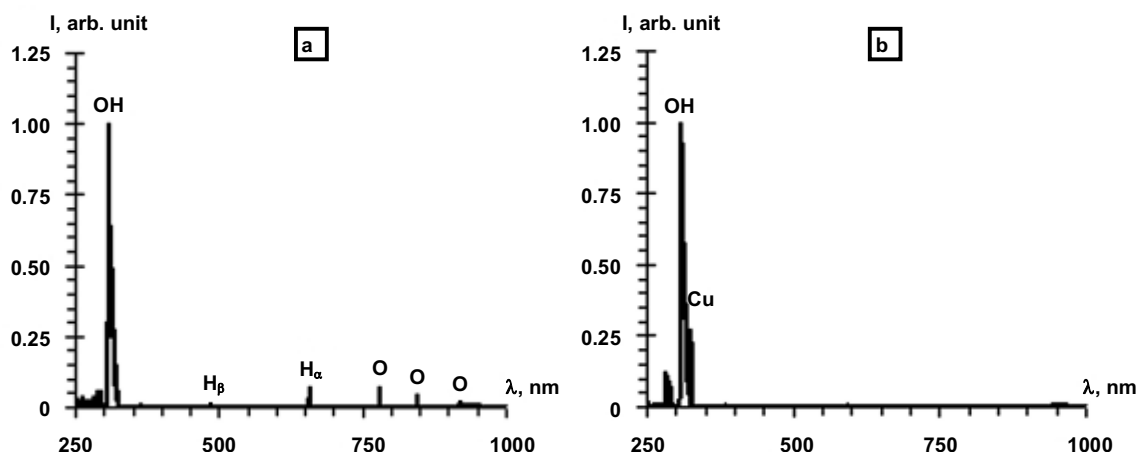
Fig. 4. Typical emission spectra of plasma inside ($Z = 2.5$ mm) (a) and outside ($Z = 30$ mm) (b) of plasma-liquid system with rotational gliding arc with liquid electrode: distilled water/air mixture

The method of comparing experimentally measured emission spectra calculated by code SPECAIR [4] to determine the temperature population of excited vibrational T_v^* and rotational T_r^* levels of hydroxyl OH was used. Comparison of the experimentally measured emission spectrum with simulated emission spectrum bands hydroxyl OH in the wavelength range 274–298 nm by code SPECAIR are shown in Fig. 5. Emission spectrum was registered in the mode – "solid" cathode, current – 380 mA, air flow – 140 cm³/s, voltage – 1.9 kV.
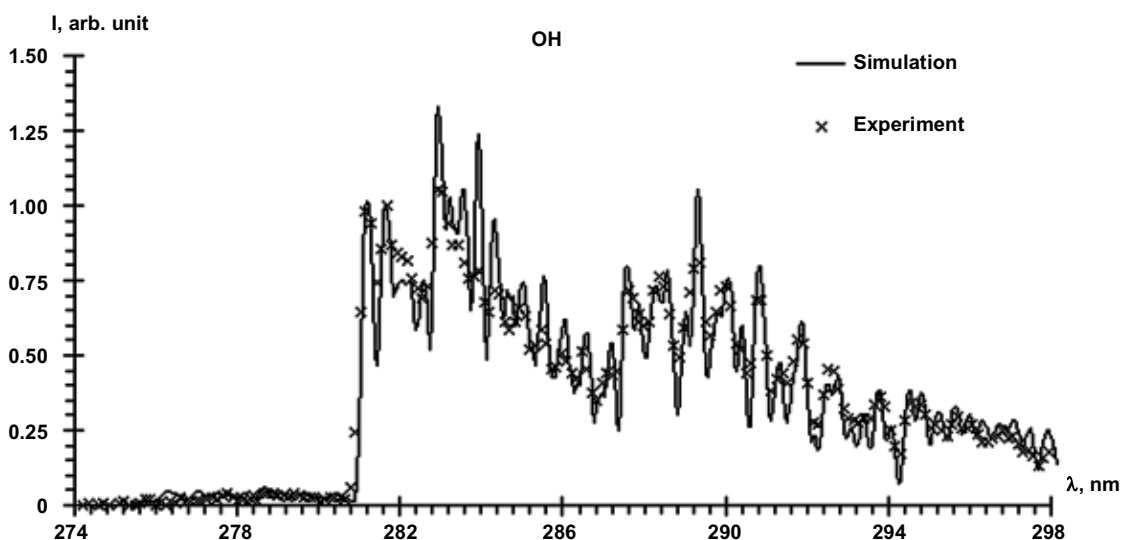

Fig. 5. Comparison of experimentally measured emission spectrum with simulated emission spectrum bands of hydroxyl OH by code SPECAIR in the wavelength range 274-298 nm. Mode is "solid" cathode, current – 380 mA, air flow – 140 cm³/s, voltage – 1.9 kV. Modeling: $T_e^*(\mathrm{O}) = 3700$ К, $T_v^*(\mathrm{OH}) = 3700$ К, $T_r^*(\mathrm{OH}) = 3700$ К

The temperature population of excited electronic levels of the oxygen atoms O, which is determined by the Boltzmann diagrams to simulate the bands of hydroxyl $\mathrm{OH(A-X)}$ was used. The temperature population of excited vibrational and rotational levels was specified by SPECAIR. The following parameters $T_e^*(\mathrm{O}) = 3700$ К, $T_v^*(\mathrm{OH}) = 3700$ К, $T_r^*(\mathrm{OH}) = 3700$ К to simulate the emission spectrum bands hydroxyl OH were used. Fig. 5 shows that the simulation matches very well with the experiment, and therefore it can be argued that the temperatures population of excited levels has the following value $T_e^*(\mathrm{O}) = 3700 \pm 400$ К, $T_v^*(\mathrm{OH}) = 3700 \pm 200$ К, $T_r^*(\mathrm{OH}) = 3700 \pm 200$ К.

Fig. 6 shows dependence of the temperature population of the excited electronic $T_e^*(\mathrm{O})$ vibrational $T_v^*(\mathrm{OH})$ and rotational $T_r^*(\mathrm{OH})$ levels from airflow. Emission spectra were registered inside of system in the center the line of sight between the liquid and the top flange. Measurements were carried out at a fixed value of current – 380 mA. Mode – "solid" cathode. The plasma at low air flow is isothermal (Fig. 6). However, the interval between the temperatures population of excited vibrational, rotational levels OH and electronic levels O increased with airflow increases. The temperature population of excited electronic levels of hydrogen H decreased with increasing of air flow.

The volume which occupies plasma inside the system is on order less than the volume of plasma torch. Temperature distribution of plasma along the torch is important, because the plasma torch is injected into the reaction chamber. Axial distribution of vibrational and rotational temperature in the plasma torch is shown in

Fig. 7. Emission spectra were registered by the line of sight. Measurements were carried out at a fixed value of current – 340 mA and air flow – 165 cm³/s. Mode – "solid" cathode. $Z = 0$ mm corresponds the measurements along the surface of the liquid, $Z = 5$ mm – along the bottom surface of the top flange, $Z = 30$ mm – along the upper surface of the upper flange. There is a one "dead" zone, in which can not be measured emission spectra. This is due peculiar structure of the upper flange.

Plasma torch reached the size to a height of 120 mm at the air flow 165 cm³/s and current 340 mA. The intensity of the bands of hydroxyl OH decreased with increasing Z. Hydroxyl bands were barely visible at the maximum accumulation for $Z = 100$ mm. However, the rotational and vibrational temperature at the values of $Z > 50$ mm from the emission spectra was difficult to determine. Since the OH bands of low intensity (274–298 nm) were used for the determination of these temperatures.
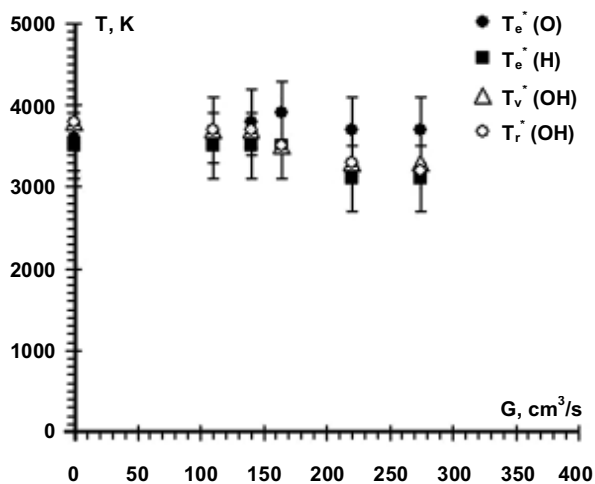

Fig. 6. Dependence temperatures population of excited electronic $T_e^*(O)$, vibrational $T_v^*(OH)$ and rotational levels of $T_r^*(OH)$ from airflow. Current – 380 mA, mode – "solid" cathode

When $Z = 0$ mm (along the surface of the liquid), the difference between $T_v^*(OH) = 3700 \pm 200$ K and $T_r^*(OH) = 3200 \pm 200$ K is 500 K, but at $Z = 5$ mm (along the bottom surface of the metal flange) they are equal within the limits of error. At $Z = 30$ mm difference between $T_v^*(OH) = 3500 \pm 200$ K and $T_r^*(OH) = 3000 \pm 200$ K is 500 K. For the $35 \le Z \le 50$ mm difference between $T_v^*(OH)$ and $T_r^*(OH)$ remains constant 700 K, but the absolute values decrease with increasing Z (Fig. 7).

According to the obtained temperatures population of excited levels and code SPECAIR unable to determine the ratio $[OH]/[O]$ between the concentration of hydroxyl OH and atomic oxygen O. Hydroxyl OH on six orders of magnitude smaller than oxygen atoms O. With increasing air flow ratio $[OH]/[O]$ begins to decrease. This ratio $[OH]/[O]$ has a maximum when the air flow 165 cm³/s. This may be due to the fact that an increasing of air flow increases the power inputted into the discharge that way fluid flow increases. With further increase flow capacity varies little, and the amount of oxygen that is introduced by

the flow increases. The concentration ratio $[H]/[O]$ by using the calculated spectra according to NIST was determined. The atoms of hydrogen $[H]$ and oxygen $[O]$ almost equal value.
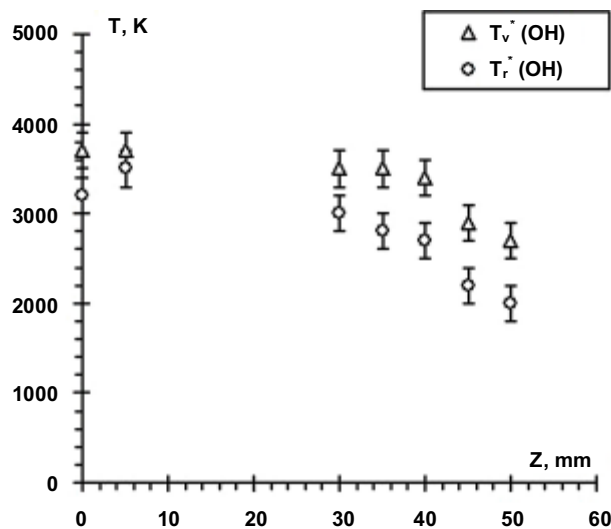

Fig.7. Axial distribution of temperatures population of excited vibrational $T_v^*(OH)$ and rotational levels of $T_r^*(OH)$. Current – 340 mA, air flow – 165 cm³/s, mode – "solid" cathode

Conclusions. Plasma of plasma-liquid system with rotational gliding arc with liquid electrode inside the chamber is isothermal $T_e^*(O) = 3700 \pm 400$ K, $T_v^*(OH) = 3700 \pm 200$ K, $T_r^*(OH) = 3700 \pm 200$ K. The interval between the temperatures population of excited vibrational, rotational levels OH and electronic levels O increased with airflow increases. Temperatures population of excited levels at air flow 275 cm³/s have the value $T_e^*(O) = 3700 \pm 400$ K, $T_v^*(OH) = 3300 \pm 200$ K, $T_r^*(OH) = 3200 \pm 200$ K.

Plasma is nonisothermic in the torch at the range of Z 30–50 mm. The difference between $T_v^*(OH)$ and $T_r^*(OH)$ is 700 K, and their absolute values decrease with height of plasma torch ($35 \le Z \le 50$ mm).

The main components of the plasma interelectrode gap are OH, O, H, and major components of the plasma torch are OH, and Cu. The concentration of hydroxyl OH on six orders of magnitude was less than the concentration of oxygen O and hydrogen H atoms.

The presence of water increases the plasma torch. This may be due to the fact that plasma generates detonating gas, which burning increases the plasma torch.

Reference
1. Beushaati B., e.a. "Density and Rotational temperature Measurements of the OH and NO Radicals Produced by a Gliding Arc in Humid Air", Plasma Chemistry and Plasma Processing. 2002. Vol. 22, no. 4. P. 553-571. 2. Kalra C.S., Kossitsyn M., Iskenderova K., Chirokov A., Cho Y.I., Gutsol A., Fridman A. Electrical discharges in the Reverse Vortex Flow – Thornado Discharges. El. Proc. Of 16th Int. Symp. on Plasma Chem. Taormina. 2003. 3. Koroteev A.S., Mironov V.M., Svirchyk Yu.S. Plasmatrons: constructions, characteristics, calculation (Book style). M. 1993. 286 p. (in Russian). 4. Laux C.O., Spence T.G., Kruger C.H., Zare R.N. Optical diagnostics of atmospheric pressure air plasma // Plasma Source Sci. Technol. 2003. Vol. 12, no. 2. P. 125–138. SPECAIR: http://www.specair-radiation.net 5. Nedybaliuk O.A., Chernyak V.Ya.,

Olszewski S.V. Plasma-Liquid System With Reverse Vortex Flow of "TORNADO" Type (TORNADO-LE) // Problems of Atomic Science and Technology. 2010. Vol. 6. P. 135–137. 6. Nedybaliuk O.A., Chernyak V. Ya., Olszewski S.V., Martysh E.V. Dynamic Plasma-Liquid

System with Discharge in Reverse Vortex Flow of "Tornado" Type // International Journal of Plasma Environmental Science & Technology. 2011. Vol. 5, no. 1, P. 20–24.

О. Недибалюк, канд. фіз.-мат. наук, В. Черняк, д-р фіз.-мат. наук,
каф. фізичної електроніки, Є. Мартиш, д-р фіз.-мат. наук, каф. медичної радіофізики,
О. Соломенко, асп., І. Федірчик, студ., каф. фізичної електроніки,
радіофізичний факультет, КНУ імені Тараса Шевченка, Київ

ПЛАЗМОВО-РІДИННА СИСТЕМА З ОБЕРТАЛЬНОЮ КОВЗНОЮ ДУГОЮ ТА РІДКИМ ЕЛЕКТРОДОМ

У роботі представлені результати дослідження обертальної ковзної дуги з рідким електродом. Досліджено спектри випромінювання плазми обертальної ковзної дуги з рідким електродом. Виміряні вольт-амперні характеристики обертальної ковзної дуги в діапазоні потоків повітря 0–220 см³/с. Визначено температури заселення збуджених електронних T_e^*, коливних T_v^* та обертових T_r^* рівнів. Досліджено розподіл цих температур вздовж плазмового факелу.

Ключові слова: плазма, обертальна ковзна дуга, рідкий електрод, плазмово-рідинна система, електричний розряд.

О. Недыбалюк, канд. физ.-мат. наук, В. Черняк, д-р физ.-мат. наук,
каф. физической электроники, Е. Мартыш, д-р физ.-мат. наук, каф. медицинской радиофизики,
Е. Соломенко, асп., И. Федирчик, студ., каф. физической электроники,
радиофизический факультет, КНУ имени Тараса Шевченка, Киев

ПЛАЗМЕННО-ЖИДКОСТНАЯ СИСТЕМА
С ВРАЩАТЕЛЬНОЙ СКОЛЬЗЯЩЕЙ ДУГОЙ И ЖИДКИМ ЭЛЕКТРОДОМ

В работе представлены результаты исследования вращательной скользящей дуги с жидким электродом. Исследованы спектры излучения плазмы вращательной скользящей дуги с жидким электродом. Измеренные вольтамперные характеристики вращательной скользящей дуги в диапазоне потоков воздуха 0–220 см3/с. Определены температуры заселения возбужденных электронных T_e^*, колебательных T_v^* и вращательных T_r^* уровней. Исследовано распределение этих температур вдоль плазменного факела.

Ключевые слова: плазма, вращающательная скользящая дуга, жидкий электрод, плазменно-жидкостная система, электрический разряд.

O. Prokopenko, Ph.D., B. Karpiak, stud., O. Sulymenko, stud.,
Department of Nanophysics and nanoelectronics, Faculty of Radiophysics,
Taras Shevchenko National University of Kyiv

DYNAMICS OF GENERALIZED PHASES IN A SYSTEM
OF TWO WEAKLY-COUPLED SPIN-TORQUE NANO-OSCILLATORS
WITH RANDOM EIGEN FREQUENCIES: THE CASE OF GLOBAL COUPLING

Dynamics of generalized phases in a system of two weakly-coupled spin-torque nano-oscillators (STNOs) with random eigen frequencies (Gaussian distribution) is analyzed. It is shown that the system dynamics is conveniently described by a complex order parameter in the scope of global coupling model. The numerical analysis of time dynamics of the modulus of complex order parameter was performed. It is shown that the synchronization of two STNOs is most effective when the amplitude of coupling Λ is big and the phase of coupling β is multiple of π.

Key words: spin-torque nano-oscillator, synchronization, coupled oscillations, random eigen frequency.

Introduction. The spin-transfer torque (STT) [1, 3, 15, 20–21] carried by a spin-polarized electric current can give rise to several types of magnetization dynamics (magnetization auto-oscillations [5–6, 8–11, 16–17] and reversal [7, 22]) and, therefore, allows one to manipulate magnetization of a nano-scale magnetic object [17].

The STT effect opens a possibility for the development of a novel type of nano-scale microwave devices – spin-torque nano-oscillators (STNOs). The practical application of STNOs faces four main problems:

- low enough operation frequencies of devices based on STNOs (typically, 1–15 GHz);
- low output microwave power (or DC power if a STNO is used as a microwave detector);
- large generation linewidth;
- imperfect manufacturing technology of STNOs.

The last three problems can be solved using the mutual phase-locking of several STNOs [6, 11, 14, 18–19]. For instance, using numerical simulations it has been demonstrated [4, 12] that the finite delay time of the coupling signal can lead to a substantial (~ 100 times) increase in the frequency band of phase-locking.

In this work we perform numerical simulations of phase-locking of two STNOs with random eigen frequencies (which are caused by the parameters spread of the STNOs due to the imperfect manufacturing technology) with

account of a delay of the coupling signal. We consider the general case of two coupled nano-contact STNOs without account of the exact type of coupling. Thus, our results are valid for different types of coupling.

Theoretical model. The dynamics of the two weakly-coupled STNO can be described by the system of coupled nonlinear equations for the complex amplitudes $c_j(t)$ of spin wave modes, excited in j-th nano-contact [2, 14, 19]:

$$\frac{dc_1}{dt} + i\,\omega_1\left(\left|c_1\right|^2\right)c_1 + \Gamma_{eff,1}\left(\left|c_1\right|^2\right)c_1 = \Omega_{12}c_2\,e^{i\beta_{1,2}}\,,$$
$$\frac{dc_2}{dt} + i\,\omega_2\left(\left|c_2\right|^2\right)c_2 + \Gamma_{eff,2}\left(\left|c_2\right|^2\right)c_2 = \Omega_{21}c_1\,e^{i\beta_{2,1}}\,, \tag{1}$$

where $j,k = \{1,2\}$, $\omega_j\left(\left|c_j\right|^2\right)$ and $\Gamma_{eff,j}\left(\left|c_j\right|^2\right)$ are the frequency and effective damping rate (that includes contribution from the positive natural damping and current-induced negative damping) of j-th mode, coupling frequencies $\Omega_{j,k}$ are defined by Eq. (6) in [19], and $\beta_{j,k}$ is the phase shift, for example, the phase shift of the spin wave (radiated by the k-th nano-contact) acquired during its propagation to the j-th nano-contact.

The system (1) without time delay ($\beta_{j,k} = 0$) was derived and analyzed in [19]. The analysis of the system (1) was